Spatial coherence effect on the low-frequency Raman scattering from metallic nanoclusters

E. Duval, H. Portales, and L. Saviot
Laboratoire de Physicochimie des Matériaux Luminescents, Université Lyon I, UMR-CNRS 5620, 43 boulevard du 11 Novembre, 69622 Villeurbanne Cedex, France

M. Fujii, K. Sumitomo, and S. Hayashi
Department of Electrical and Electronics Engineering, Faculty of Engineering, Kobe University, Rokkodai, Nada, Kobe 657-8501, Japan
(Received 25 July 2000; published 25 January 2001)

The low-frequency plasmon-resonant Raman scattering by the vibrational modes of silver nanoclusters embedded in amorphous SiO_2 films is studied experimentally and theoretically. By electron microscopy it is observed that the concentration of defects in nanocrystals decreases and the intensity of Raman scattering increases by thermal annealing. It is shown that the degree of spatial coherence inside clusters has a strong effect on the Raman intensity and on its frequency dependence.

DOI: 10.1103/PhysRevB.63.075405 PACS number(s): 61.46.+w, 36.20.Ng, 63.20.Pw

I. INTRODUCTION

Nanocrystals of metal, in particular of silver or gold, embedded in insulating matrices strongly absorb the light by exciting electronic surface plasma dipolar oscillations. This strong absorption and the surface plasmons themselves have been the subject of extensive research, which was often motivated by the optical nonlinear properties it produces.[1] Another consequence of the strong absorption is the relatively intense Raman scattering by the vibrations of silver nanoclusters.[2–5] For an approximately spherical shape, the cluster vibrations are characterized by the quantum numbers l and m (which characterize the spherical harmonic functions related to the symmetry group of the sphere) and the index $n \geqslant 1$ labeling—in increasing order of frequency—the sequence of the eigenmodes for given l and m values. It was shown by group theory that, among the two types (torsional and spheroidal) of modes, only the $l=0$ spherical and $l=2$ quadrupolar spheroidal modes can scatter the light.[6] Only the quadrupolar modes were experimentally observed.[2,5] This Raman selection rule can be justified by the cubic symmetry of the internal lattice and assuming a dipole-induced dipole mechanism of light scattering.[7] However, the characteristics of the Raman spectra (in particular the depolarization ratio) are not in agreement with this interpretation.[5] They were properly explained by the resonance of the Raman light excitation with the surface dipolar plasmons.[5]

The effect of resonance depends on the strength of the plasmon-phonon coupling. The dipolar surface plasmon, which corresponds to a large oscillating electric dipole, is characterized by the quantum number $L=1$. From group theory, the coupling of the dipolar plasmon is allowed with the $l=0$ and $l=2$ phonons. However, as noted earlier by Gersten *et al.*,[9] a spherical vibrational oscillation ($l=0$) is not expected to produce significant modulation of the electric dipole, so that the Raman scattering by the $l=0$ mode will be very low, if visible. Conversely, the quadrupolar or ellipsoidal distorsions are strongly coupled to the dipolar plasmon,[9] so that the Raman scattering by the $l=2$ modes is strongly enhanced by plasmon resonance.

In this paper, the effect of annealing on the plasmon-resonant vibrational Raman scattering from silver nanoclusters embedded in amorphous silica films will be compared to electron microscopy observations. The increase and the change of the frequency dependence of the Raman intensity by annealing will be related to the improvement of crystallinity or spatial coherence inside clusters. A theoretical model of Raman scattering from nanoclusters will support the observations and will show that the effect of crystallinity on Raman scattering can be huge.

II. EXPERIMENT

Samples were prepared by a rf cosputtering method similar to that described in Ref. 3. The used substrates were Si wafers or fused quartz plates. The thickness of the films is about 400 nm. During the sputtering, the substrates were cooled by circulating water, and the temperature was kept lower than 50°C. After the sputtering, the samples were cut into several pieces, and some of them were annealed in N_2 gas ambient for 30 min at 800°C. In order to determine the size distribution, shape, and crystallinity of Ag particles, the cross sections of all the samples (both the as-deposited and annealed) were observed by high-resolution transmission electron microscopy (HRTEM) (JEM-2010 of JEOL). For the cross-section HRTEM observations, samples were thinned by using a standard mechanical and Ar-ion thinning technique. The Raman spectra were recorded with a five-grating monochromator. The high resolution and rejection of this setup make it possible to observe the low-frequency Raman signal close to the Rayleigh line. The incoming light beam was at grazing incidence and the scattered one was detected at about $\pi/2$ with respect to excitation.

In a previous work[5] it was shown that blue light is Raman-scattered mainly by the fivefold-degenerate quadrupolar vibrations of spherical clusters, and red light by the nondegenerate vibration of ellipsoidal ones. This is due to the fact that an ellipsoidal distortion affects both the dipolar plasmon and the quadrupolar vibrational modes; the former is split into a nondegenerate mode (which in turn is shifted to low energies for a prolate shape) and a twofold-degenerate mode, while the latter are split into a nondegenerate mode

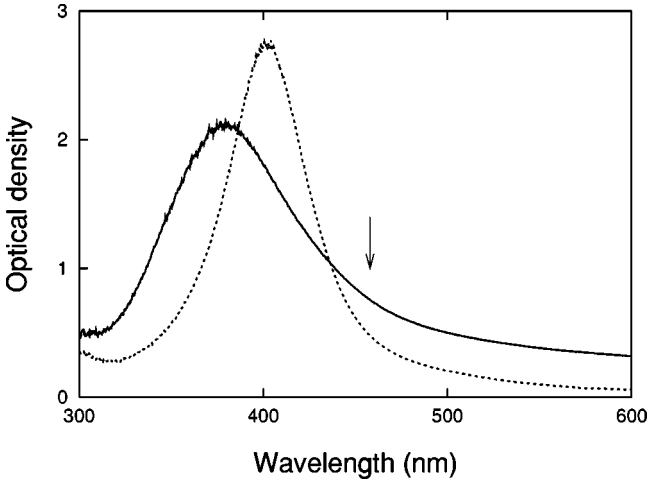

FIG. 1. Absorption spectra of the as-deposited (continuous line) and annealed (dashed line) films. The position of the 457.9-nm line is indicated by the arrow.

and two twofold-degenerate modes. Furthermore, the nondegenerate vibrational mode is coupled to the nondegenerate plasmon. Consequently, the resonant Raman scattering of red light (produced by the nondegenerate quadrupolar mode) occurs by exciting the nondegenerate plasmon of ellipsoidal clusters. Conversely, the resonant Raman scattering of blue light (produced by the fivefold-degenerate quadrupolar modes) occurs principally in spherical clusters by exciting the threefold-degenerate plasmon.[5] This picture was confirmed by the measurement of the depolarization ratio, I_{VH}/I_{VV}, performed with parallel (VV) or perpendicular (VH) excitation and detection polarizations. We found $I_{VH}/I_{VV} \simeq 0.65$ with the 457.9-nm Ar^+ laser line and $I_{VH}/I_{VV} \simeq 0.4$ with the 647.1-nm Kr^+ line. The theoretical values are, respectively, 3/4 for the spherical clusters and 1/3 for the ellipsoidal ones.[2,5] It can therefore be concluded that by excitation at 457.9 nm the scattering occurs principally by the quadrupolar modes of the spherical clusters.

The absorption spectra of the as-deposited and annealed films are compared in Fig. 1. Several effects due to annealing are observed, in particular a narrowing and a shift of the plasmon band from 380 nm to 400 nm. These effects can be partially interpreted by assuming narrower size and shape distributions of clusters and an improved cluster-matrix contact after annealing. In this paper, only the Raman spectra obtained with the 457.9-nm line will be considered.

The spectra of the as-deposited and annealed films are shown in Fig. 2. It is observed that after annealing the Raman peak is shifted from 14.7 cm^{-1} to 7.9 cm^{-1}, furthermore its width is narrowed and the intensity is increased by a factor close to 10, although the absorption at 457.9 nm is weaker in the annealed film. On the other hand, as observed by electron microscopy, the cluster radius at the maximum of the size distribution increases from 1.9 nm to 2.2 nm by annealing. The shift of the Raman peak cannot be accounted for by such small increase of cluster size alone.

The HRTEM images show a better crystallization of the clusters after annealing (Fig. 3). In the as-deposited film, one observes many more nanocrystals with defects, such as grain

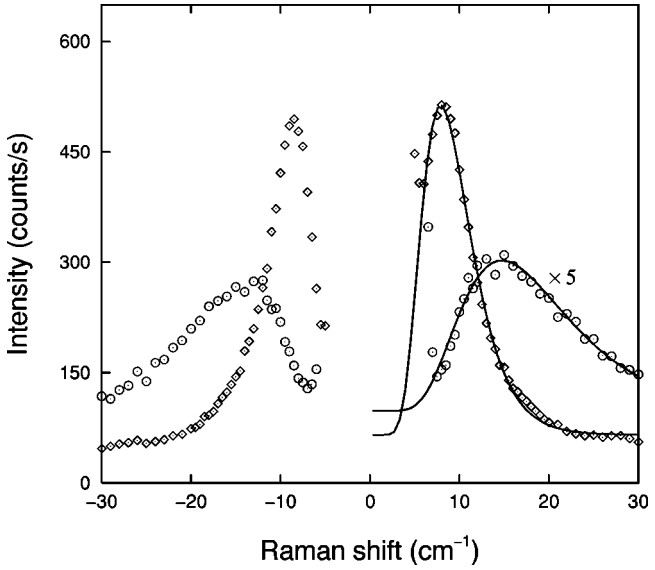

FIG. 2. Raman scattering spectra from the as-deposited (circles, the intensity is multiplied by 5) and annealed (diamonds) films. The continuous lines are the fits by the log-normal distributions plus a constant.

boundaries. The order or crystallinity is increased by annealing. To control the effect of crystallinity on light scattering, the position and shape of the Raman peak will be compared to the cluster size (or diameter) distribution, $F(D)$, that was determined by electron microscopy.

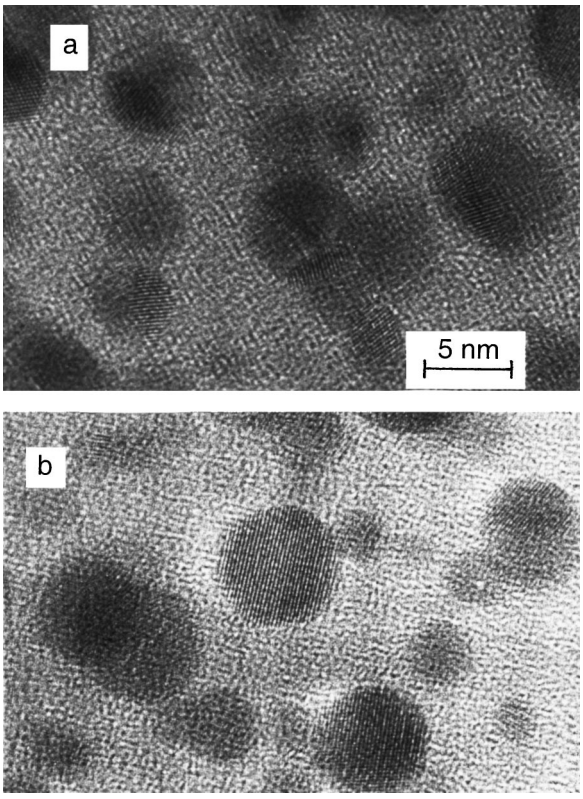

FIG. 3. Images of Ag nanoclusters obtained by high-resolution transmission electron microscopy: (a) as-deposited sample, (b) annealed sample.

III. SPATIAL COHERENCE EFFECT ON RAMAN SCATTERING: THEORY

Looking at the HRTEM images, one would expect a simple explanation for the difference in the vibrational Raman spectra of, respectively, the as-deposited and the annealed films. The Raman scattering from as-deposited samples would be due to the vibrations of the grains and not to those of the whole cluster. In other words, there would be no correlation between the vibrations of different grains in a cluster. Consequently, the Raman intensity should be compared with the size distribution of the grains, and not with that of the clusters. It was shown theoretically[8] and confirmed experimentally[2,5] that the frequency ω of the quadrupolar vibrational modes is inversely proportional to the diameter $2a$ of the vibrating nanoparticle or nanograin:

$$\omega(\mathrm{cm}^{-1}) = 0.85 \frac{v_t}{2ac}, \tag{3.1}$$

v_t being the transverse sound velocity in the metal and c the vacuum light speed. From Eq. (3.1), the shift of the Raman peak from 14.7 cm^{-1} to 7.9 cm^{-1} after annealing (Fig. 2) would be explained by assuming that the vibrating objects are the grains ($2a<D$) in the as-deposited films and the entire clusters ($2a \simeq D$) in the annealed films, as the grain boundaries disappear with annealing. However, as we will show later, this explanation does not agree with the increase of the Raman peak intensity, which is observed after annealing (Fig. 2). It will be shown that the difference between the Raman peaks of the as-deposited and annealed films is produced by the improvement of the cluster crystallinity, or spatial coherence, by heat treatment.

The intensity of light scattered by a cluster of volume V_c is given by the Raman tensor $\delta I_{\alpha\beta}(\omega)$, which is the Fourier transform of the correlation function of the space- and time-dependent fluctuation $\delta\chi$ of the electric susceptibility χ:[10]

$$\delta I_{\alpha\beta}(\omega) = \frac{1}{2\pi V_c} \int_{-\infty}^{+\infty} dt\, e^{-i\omega t} \int\int_{V_c} d\mathbf{r}_1 d\mathbf{r}_2 \times \exp[-i\mathbf{k}(\mathbf{r}_1-\mathbf{r}_2)] \langle \delta\chi_{\alpha\beta}(\mathbf{r}_1,t)\, \delta\chi_{\alpha\beta}(\mathbf{r}_2,0)\rangle, \tag{3.2}$$

where α and β are the polarizations of the incident and scattered lights, respectively, $\mathbf{r}_1$ and $\mathbf{r}_2$ are the position vectors of two different points in the cluster, and $\langle\cdots\rangle$ is the thermal average correlation function. Since, on the one hand, the product of the light momentum transfer $\mathbf{k}$ by $(\mathbf{r}_1-\mathbf{r}_2)$ is very small, and, on the other hand, the wave vector of the cluster surface mode observed by Raman scattering is equal to zero, the Raman scattering from a nanocluster is independent of $\mathbf{k}$ ($\exp[-i\mathbf{k}(\mathbf{r}_1-\mathbf{r}_2)] \simeq 1$). Considering the Raman scattering by only one cluster surface mode of frequency ω, among the fivefold-degenerate quadrupolar ones, it is obtained for Stokes scattering:

$$\delta I_{\alpha\beta}(\omega) = \frac{1}{V_c} \frac{n(\omega)+1}{\omega} \times \int\int d\mathbf{r}_1 d\mathbf{r}_2 \langle \delta\chi_{\alpha\beta}(\mathbf{r}_1,\omega)\, \delta\chi_{\alpha\beta}(\mathbf{r}_2,\omega)\rangle, \tag{3.3}$$

where $\langle\cdots\rangle$ is the space correlation function and $n(\omega)$ is the Bose factor. In the case of resonant Raman scattering, $\delta\chi(\mathbf{r})$ is proportional to the amplitudes of both the plasmon wave function and the vibrational wave function and to the plasmon-phonon coupling coefficient at the position $\mathbf{r}$ in the cluster. In a perfectly crystallized cluster, the spatial coherence is reflected on the plasmon and phonon states, on the plasmon-phonon coupling coefficient, and consequently on $\delta\chi(\mathbf{r})$. Related to the crystalline order, the correlation function is equal to 1 in a perfectly crystallized cluster, and therefore

$$\delta I^{\mathrm{coh}}_{\alpha\beta}(\omega) = \frac{n(\omega)+1}{\omega V_c} \int d\mathbf{r}_1\, \delta\chi_{\alpha\beta}(\mathbf{r}_1,\omega) \int d\mathbf{r}_2\, \delta\chi_{\alpha\beta}(\mathbf{r}_2,\omega) \tag{3.4}$$

or

$$\delta I^{\mathrm{coh}}_{\alpha\beta}(\omega) = \frac{n(\omega)+1}{\omega} V_c \langle \delta\chi_{\alpha\beta}(\omega)\rangle^2, \tag{3.5}$$

where $\langle\cdots\rangle$ is the mean value. The coherence volume is equal to V_c. In comparison with this specified coherence, defects such as grain boundaries bring a spatial incoherence reflected on the susceptibility fluctuation, which takes the form $\delta\chi(\mathbf{r})e^{i\varphi(\mathbf{r})}$, where $\varphi(\mathbf{r})$ is a phase depending on the disorder in the cluster. It follows that

$$\delta I_{\alpha\beta}(\omega) = \frac{n(\omega)+1}{\omega V_c} \int\int d\mathbf{r}_1 d\mathbf{r}_2\, \delta\chi_{\alpha\beta}(\mathbf{r}_1,\omega)\, \delta\chi_{\alpha\beta}(\mathbf{r}_2,\omega) \times \exp i[\varphi(\mathbf{r}_1)-\varphi(\mathbf{r}_2)], \tag{3.6}$$

where $\exp i[\varphi(\mathbf{r}_1)-\varphi(\mathbf{r}_2)]$ is the correlation function.[11,12] In the case of complete incoherence, the correlation function becomes $\delta(\mathbf{r}_1-\mathbf{r}_2)$ and

$$\delta I^{\mathrm{incoh}}_{\alpha\beta}(\omega) = \frac{n(\omega)+1}{\omega V_c} v \int d\mathbf{r}[\delta\chi_{\alpha\beta}(\mathbf{r},\omega)]^2. \tag{3.7}$$

In this equation, v is an atomic volume. By integration, one obtains

$$\delta I^{\mathrm{incoh}}_{\alpha\beta}(\omega) = \frac{n(\omega)+1}{\omega} v \langle[\delta\chi_{\alpha\beta}(\omega)]^2\rangle. \tag{3.8}$$

The mean value $\langle[\delta\chi_{\alpha\beta}(\omega)]^2\rangle$ is for the ordered system, consequently in resonant Raman scattering, $\langle[\delta\chi_{\alpha\beta}(\omega)]^2\rangle = \langle\delta\chi_{\alpha\beta}(\omega)\rangle^2$, and one obtains

$$\delta I^{\mathrm{coh}}_{\alpha\beta}(\omega) = \delta I^{\mathrm{incoh}}_{\alpha\beta}(\omega) N, \tag{3.9}$$

N being the number of atoms in the cluster. This equation shows the possible huge effect of the spatial coherence or

crystallinity on the Raman scattering from the studied silver nanoclusters, which contain about 2000 atoms. In the general case, the volume of coherence is equal to ϑV_c, with $v/V_c \leqslant \vartheta \leqslant 1$, and V_c in Eq. (3.5) is replaced by ϑV_c. Because one expects that the probability to find defects in the cluster increases with the cluster size, the spatial coherence coefficient ϑ is believed to be dependent on the cluster size, i.e., from Eq. (3.1), on ω. As $V_c \sim D^3$ and from Eq. (3.1) $D^3 \sim \omega^{-3}$, the frequency dependence of the Raman scattering from a cluster is, in the general case, the following:

$$\delta I_{\alpha\beta}(\omega) \propto \delta I_{\alpha\beta}^{\mathrm{incoh}}(\omega) \frac{\vartheta(\omega)}{\omega^3}. \tag{3.10}$$

It should be noted that the relation between ϑ and ω is not unique because the spatial coherence volume in clusters of the same size can vary from one cluster to another. This is why a mean spatial coherence coefficient will be introduced.

From now on, we will drop the polarization indexes α and β because, from experiment, they have no effect on the variation of the Raman intensity with crystallinity. As verified by experiment, the homogeneous Raman linewidth related to the phonon lifetime is much narrower than the frequency distribution $F(\omega)$ deduced from the cluster size distribution $F(D)$ by Eq. (3.1). From these considerations, the total intensity $I(\omega)$ is written as

$$I(\omega) \propto \delta I^{\mathrm{incoh}}(\omega) \frac{\theta(\omega)}{\omega^3} F(\omega). \tag{3.11}$$

In this expression, the new spatial coherence coefficient $\theta(\omega)$ is the mean value of $\vartheta(\omega)$ for the nanocrystals vibrating at frequency ω. This distinction between $\vartheta(\omega)$ and $\theta(\omega)$ is necessary, because, as mentioned above for a given cluster volume or frequency, the degree of coherence can change from one cluster to another.

IV. DISCUSSION

It is useful to consider the shape of the Raman peak before discussing the spatial coherence in clusters. In Fig. 2, the Raman intensities, $I(\omega)$, are well fitted by a log-normal distribution. On the other hand, the size distribution, $F(D)$, determined by electron microscopy is also log-normal. Furthermore, the standard deviations σ for $I(\omega)$ and $F(D)$, respectively, are very close. Since ω is related to D [Eq. (3.1)], there is certainly a remarkable relation between $I(\omega)$ and $F(D)$. To find this relation, let us recall the properties of the log-normal distribution. The log-normal distribution of a variable x has the following expression:

$$F(x) = \frac{1}{(2\pi)^{1/2} \ln \sigma} \exp\left(- \frac{(\ln x - \ln \bar{x})^2}{2 \ln^2 \sigma} \right), \tag{4.1}$$

where $\bar{x}$ is the most probable x. It is easily found that $x^n F(x)$ and $F(x^{-1})$ are also log-normal distributions with the same standard deviation σ. As a consequence, and from Eq. (3.1), $F(\omega)$ and $\omega^n F(\omega)$ are also log-normal with the same standard deviation as $F(D)$. We conclude that the frequency dependence of $I(\omega)$ is the same as that of $\omega^n F(\omega)$. Such a frequency dependence was already found experimentally in a previous work.[5] It is also interesting to note that $F(D)$, $F(D^{-1})$, and $F(\omega)$ are mathematically related: $F(\omega)\delta(\omega) = F(D^{-1})\delta(D^{-1}) = F(D)\delta(D)$, $\delta(x)$ representing a small positive variation of x. From this relation and Eq. 3.1, one obtains $F(\omega) \propto F(D^{-1})$ and $F(\omega) \propto \omega^{-2} F(D)$.

For the log-normal distributions that fit the experimental intensities in Fig. 2, we find $\sigma = 1.51$ for the as-deposited films and $\sigma = 1.42$ for the annealed ones. Such values of σ are within the interval ($\sigma = 1.48 \pm 0.12$) of those of Granqvist and Buhrmann for the log-normal distributions of metallic nanoparticles obtained by evaporation and deposition on a copper plate.[13] These authors interpreted their observed particle size distributions by a coalescence growing process.[13] It is likely that such a coalescence process exists also for our clusters and takes place after sputtering and deposition of small aggregates.

A critical remark should be made about $F(\omega)$, which could apparently lead to the explanation of the Raman peak shift observed after annealing (Fig. 2), as suggested at the beginning of Sec. III. The distribution $F(\omega)$ for the as-deposited film could correspond to the grain size distribution, and not directly to the $F(D)$ of clusters. One may imagine that the grain size distribution differs from $F(D)$ by a simple translation towards smaller sizes. By annealing, the grain boundaries disappear and therefore the Raman peak would shift to lower frequencies like $F(\omega)$. However, this explanation must be rejected for the following reason. In this interpretation, the frequency dependence of $I(\omega)$ is the same for the as-deposited film and for the annealed one [$\omega^n F(\omega)$], so that the integrated intensity of the Raman peak should increase with the number of vibrating objects, grains or clusters. As a consequence, the Raman intensity, like the number of grains or clusters, should be larger in the as-deposited film. This is just the opposite of what is observed (Fig. 2).

To test the spatial coherence in clusters, the Raman intensity, $I(\omega)$, was compared with the size distribution, $F(D)$, determined by electron microscopy. In Fig. 4, the frequency at the maximum of $I(\omega)\omega^\alpha$ is plotted against $1/D_{\max}$, $D_{\max}$ being the diameter at the maximum of $F(D)$. For the as-deposited samples, one sees in Fig. 4 that the two experimental points are aligned with the origin of coordinates for $\alpha = 0$. From Eq. (3.1), this value of α indicates that $I(\omega) \propto F(D)$. At this point, it is remarked that the same size dependence was found for the silver nanoclusters deposited by laser evaporation simultaneously with the electron evaporation of the alumina matrix.[5] The experimental points of the annealed samples are well aligned with the origin, and with the just considered points of the as-deposited samples, for $\alpha = 2$. On the other hand, as seen in Fig. 4, the experimental points are not aligned with the origin for other α values. The straight line in Fig. 4 is very interesting for two reasons: (i) it shows that for the annealed samples $I(\omega) \propto F(D)/\omega^2$; (ii) the sound velocity given by the slope [see Eq. (3.1)] of the straight line in Fig. 4 is the same for the as-deposited and the annealed silver clusters, $v_t = 1710$ m/s. This sound velocity in nanocrystals is very close to the macroscopic one, v_t

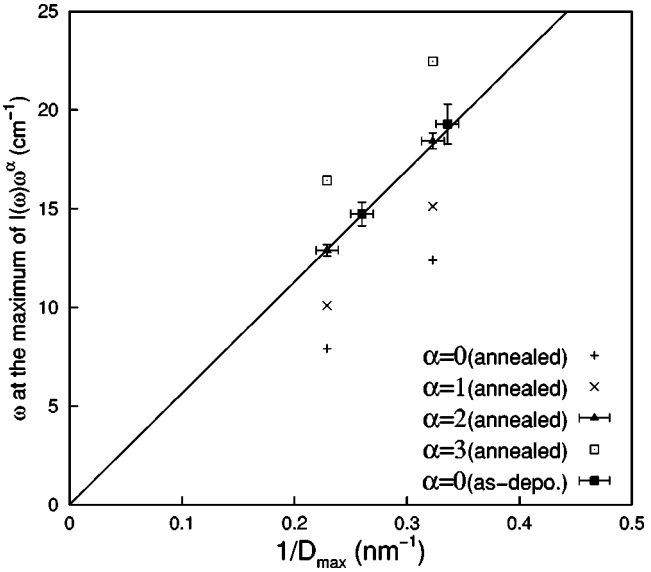

FIG. 4. The frequency at the maximum of $I(\omega)\omega^{\alpha}$ is plotted against the inverse of the diameter, $1/D_{\max}$, at the maximum of the cluster size distribution, $F(D)$.

$=1660$ m/s.[14] Such a value makes us confident of the different frequency dependence found for the two different samples.

To confirm the different cluster size dependence of $I(\omega)$ for the as-deposited and for the annealed films, the shapes of the Raman bands were compared with the inverse size distributions $F(D^{-1})$. From $I(\omega)\propto F(D)$ and Eq. (3.1), one obtains $I(\omega)/\omega^2\propto F(D^{-1})$ for the as-deposited samples, and from $I(\omega)\omega^2\propto F(D)$, $I(\omega)\propto F(D^{-1})$ for the annealed samples. The comparison is shown in Fig. 5. Very good fits of the Raman intensities by the inverse size distributions, according to the above relations, are found for $v_t=1765$ m/s (as-deposited) and $v_t=1625$ m/s (annealed). Therefore, Fig. 5 confirms the straight line in Fig. 4.

Figures 4 and 5 compared with expression (3.11) show that the frequency dependence of the spatial coherence coefficient $\theta(\omega)$ for the annealed sample is approximately proportional to that of the as-deposited film divided by ω^2. This means that, going from the as-deposited to the annealed film, one does not go from a complete incoherence to a perfect coherence, or to a partial coherence independent of the cluster size. If this were the case, the frequency dependence of $\theta(\omega)$ would be divided by ω^3, after annealing. This frequency behavior is not at variance with the HRTEM observations. A first indication, which can be verified in Fig. 3, is the presence of defective nanocrystals even after annealing. Second, it was observed that the smaller the clusters are, the less defective they are. Third, whatever the cluster size D, the number of nondefective nanocrystals increases with annealing, and furthermore (or consequently) the number of nondefective nanocrystals increases more slowly with D^{-1} or ω after annealing. These observations are only qualitative. To sum up, they convey two important pieces of information: (i) The total volume of coherence summed on all the nanocrystals increases with annealing, and this explains the increase of the Raman intensity with annealing (Fig. 2); (ii)

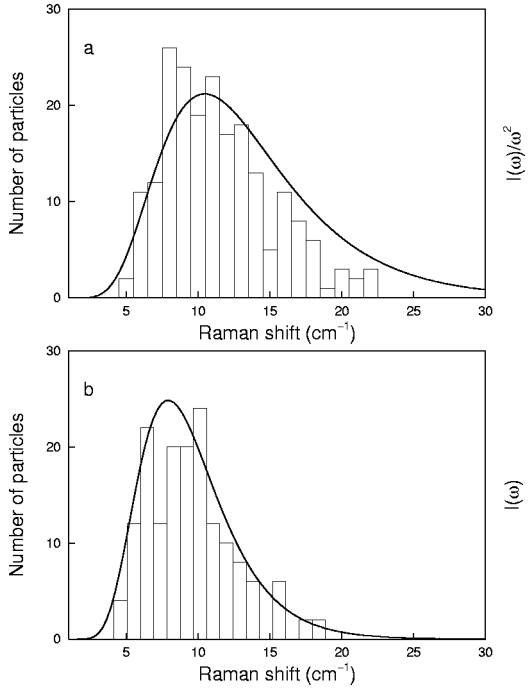

FIG. 5. Superposition of the inverse cluster radius distribution, $F(D^{-1})$, (a) on the Raman intensity divided by ω^2, $I(\omega)/\omega^2$, for the as-deposited film; (b) on $I(\omega)$ for the annealed film.

the spatial coherence coefficient $\theta(\omega)$ increases more slowly with ω or D^{-1} after annealing. As a matter of fact, $\theta(\omega)$ is assumed to have a power-law frequency dependence:

$$\theta(\omega)\propto\omega^{x}. \tag{4.2}$$

From Eq. (4.2) and from Figs. 4 and 5, we see that the annealing reduces x of two units, and this is a quantitative measure of the frequency dependence variation with annealing. From Eq. (3.1), the reduction of x confirms that the spatial coherence decreases more slowly (with cluster size) after annealing than before. Let us remark that since the frequency dependence of $\delta I^{\mathrm{incoh}}(\omega)$ in Eq. (4.1) is not known, it is not possible to determine x, but only its variation. *A priori*, the value of this exponent is not limited and may be fractional.

V. CONCLUSION

The comparison between as-deposited and annealed films evidences the effect of crystallinity or spatial coherence on the intensity of the low-frequency Raman scattering from silver nanoclusters. The increase of spatial coherence in single nanoclusters is reflected by an increase of the Raman intensity, which can be huge. On the other hand (as is easily understandable and confirmed by the electron microscopy observations), the crystallinity of a cluster decreases by increasing its size. As a consequence, due to the relationship that links the size and the vibrational frequency, the variation of crystallinity with cluster size contributes to the frequency dependence of the Raman intensity. Furthermore, as the annealing reduces the amplitude of the crystallinity variation with the cluster size, the corresponding variation of the Ra-

man intensity with frequency is weaker in the annealed samples. This explains the shift of the Raman peak to lower frequency after annealing: in the case of the as-deposited samples, the smallest nanoclusters mainly contribute to Raman scattering because of the weak probability of having defects inside, and consequently the frequency of the Raman peak is relatively high. By annealing, the defects are annealed for almost all sizes, so that the relative contribution of the largest nanoclusters to the Raman intensity increases with spatial coherence, and the Raman peak is shifted to lower frequency. However, we would like to stress again that the normal vibrational modes are the modes of the complete cluster, even with defects like grain boundaries inside. The determination of the cluster spatial coherence effect on the frequency dependence of Raman intensity is necessary to determine the contribution of the plasmon resonance to this frequency dependence, i.e., to know the frequency dependence of $\delta I^{\mathrm{incoh}}(\omega)$. Finally, on the basis of the results obtained for the resonant Raman scattering, we expect that a higher degree of crystallinity will result in better nonlinear optical properties of the nanoclusters.

ACKNOWLEDGMENTS

The authors thank M. Montagna, G. Viliani, B. Champagnon, and J. Lermé for valuable discussions.

[1] U. Kreibig and M. Vollmer, *Optical Properties of Metal Clusters* (Springer, New York, 1995).
[2] G. Mariotto, M. Montagna, G. Viliani, E. Duval, S. Lefrant, E. Rzepka, and C. Mai, Europhys. Lett. **6**, 239 (1988).
[3] M. Fujii, T. Nagareda, S. Hayashi, and K. Yamamoto, Phys. Rev. B **44**, 6243 (1991).
[4] M. Ferrari, L.M. Gratton, A. Maddalena, M. Montagna, and C. Tosello, J. Non-Cryst. Solids **191**, 101 (1995).
[5] B. Palpant, H. Portales, L. Saviot, J. Lermé, B. Prével, M. Pellarin, E. Duval, A. Perez, and M. Broyer, Phys. Rev. B **60**, 17 107 (1999).
[6] E. Duval, Phys. Rev. B **46**, 5795 (1992).
[7] M. Montagna and R. Dusi, Phys. Rev. B **52**, 10 080 (1995).
[8] E. Duval, A. Boukenter, and B. Champagnon, Phys. Rev. Lett. **56**, 2052 (1986).
[9] J.I. Gersten, D.A. Weitz, T.J. Gramila, and A.Z. Genack, Phys. Rev. B **22**, 4562 (1980).
[10] J. Jäckle, in *Amorphous Solids* (Springer, Berlin, 1981), p. 135.
[11] P. Beckmann and A. Spizzichino, in *The Scattering of Electromagnetic Waves From Rough Surface* (Pergamon, New York, 1963).
[12] E. Duval, N. Garcia, A. Boukenter, and J. Serughetti, J. Chem. Phys. **99**, 2040 (1993).
[13] C.G. Granqvist and R.A. Buhrman, Solid State Commun. **18**, 123 (1976).
[14] *Chronological Scientific Tables*, edited by National Astronomical Observatory (Maruzen, Tokyo, 1991).